



## Interactions of persistent slip bands with a grain boundary on the common primary slip plane in a copper bicrystal

Z. F. ZHANG<sup>†</sup> and Z. G. WANG

State Key Laboratory for Fatigue and Fracture of Materials, Institute of Metal Research, Chinese Academy of Sciences, Shenyang, 110015, PR China

[Received in final form 4 November 1999 and accepted 9 November 1999]

### ABSTRACT

In this letter, the dislocation patterns on the common primary slip plane in a fatigued  $[\bar{1}34]$ – $[18\bar{2}7]$  copper bicrystal with a  $\Sigma = 19b$  grain boundary (GB) have been investigated using the electron channelling contrast technique in a scanning electron microscope. The results show that the two-phase dislocation structure, such as veins and persistent slip band (PSB) walls, embedded within veins, can be clearly seen on the common primary slip plane. In particular, the interactions of PSBs with the GB are clearly revealed. It is found that there are three kinds of interaction mode between the GB and the dislocations during cyclic deformation, and those are discussed. It is suggested that the dislocations carried by PSBs cannot transfer through the GB continuously even though the bicrystal has a common primary slip plane and its surface slip bands are continuous across the GB.

### § 1. INTRODUCTION

During cyclic deformation of copper and nickel single crystals, a large fraction of plastic strain is carried by the so-called persistent slip bands (PSBs), which consist of thin lamellae transferring through the specimens in the bulk. In particular, the PSBs are composed of nearly parallel and narrow dislocation walls arranged with fairly equal spacing perpendicular to the primary Burger vector and are embedded in a matrix structure of loop patches. This feature has been explained by a two-phase model (PSBs and matrix) according to Winter (1974) and Finney and Laird (1975). The peculiar dislocation arrangement of the PSB lamellae has been extensively studied by transmission electron microscopy (TEM) and described in several review articles (Laird *et al.* 1986, Basinski and Basinski 1992). However, TEM investigations require thin-foil specimens and only a relatively small area can be investigated. Recently, the electron channelling contrast (ECC) technique in a scanning electron microscope has been successfully applied in studying the dislocation patterns in deformed metals (Dudarev *et al.* 1999, Wilkinson and Hirsch 1995, 1997), such as stainless steel (Zauter *et al.* 1992), nickel (Schwab *et al.* 1996, 1998, Bretschneider *et al.* 1997), copper (Ahmed *et al.* 1997, Gong *et al.* 1997, Melisova *et al.* 1997, Li *et al.* 1998) aluminium (Mitchell and Day 1998). It has been generally recognized that the scanning electron microscopy (SEM)–ECC technique can reveal information which is difficult to achieve by conventional TEM techniques. For example, it allows the

<sup>†</sup> Author for correspondence. E-mail: zhzhzhang@imr.ac.cn.

observations of dislocation patterns over the whole cross-section of the specimen, and especially at some special sites, such as in the vicinity of a grain boundary (GB) (Hu *et al.* 1998, Zhang and Wang 1998, Zhang *et al.* 1999), deformation bands (Gong *et al.* 1997, Melisova *et al.* 1997, Li *et al.* 1998) and a crack (Wilkinson *et al.* 1997). In our previous work, the dislocation patterns near the large-angle and small-angle GBs in fatigued copper bicrystals have been investigated by this technique (Hu *et al.* 1998, Zhang and Wang 1998, Zhang *et al.* 1999). In particular, in a  $[\bar{1}34]$ - $[18\bar{2}7]$  copper bicrystal, the two-component crystals possess a common primary slip plane and the interaction of PSBs with the GB was not clearly revealed throughout the depth of the specimen (Zhang *et al.* 1999). It is necessary to explore the distribution of dislocation patterns near the GB on the common primary slip plane so that the intergranular fatigue cracking mechanism may be clarified. In this letter, we focus attention on the observations on the common primary slip plane to reveal the interactions of the coplanar PSBs with the GB using the SEM-ECC technique by polishing away the specimen layer by layer.

## § 2. EXPERIMENTAL PROCEDURE

In our previous work (Zhang *et al.* 1999), a  $[\bar{1}34]$ - $[18\bar{2}7]$  copper bicrystal with a common primary slip plane was fabricated. By the electron back-scatter diffraction (EBSD) technique, the crystallographic relation of the bicrystal was carefully determined. It was found that the common rotation axis between the two-component crystals was in the  $[111]$  direction, which is also the normal to the common primary slip plane in the bicrystal. The rotation angle around the  $[111]$  rotation axis between the crystals G1  $[\bar{1}34]$  and G2  $[18\bar{2}7]$  was  $46.2^\circ$ , thereby forming a  $\Sigma = 19b$  coincidence GB. Figure 1 shows the crystallographic relations on the common primary slip plane of the bicrystal. Clearly, the interaction angle  $\theta$  between the primary Burgers vectors  $\mathbf{b}_1$  and  $\mathbf{b}_2$  of the crystals G1 and G2 should be equal to  $13.8^\circ$  (i.e.  $60^\circ - 46.2^\circ$ ). However, the crystallographic orientations of the GB planes of the two crystals were difficult to determine. The slip morphology and dislocation patterns on the surfaces of the bicrystal have been reported previously (Zhang *et al.* 1999). The primary slip planes of the two crystals in the bicrystal are coplanar and can be sectioned according to the surface slip traces after cyclic deformation. Since the PSB lamellae are

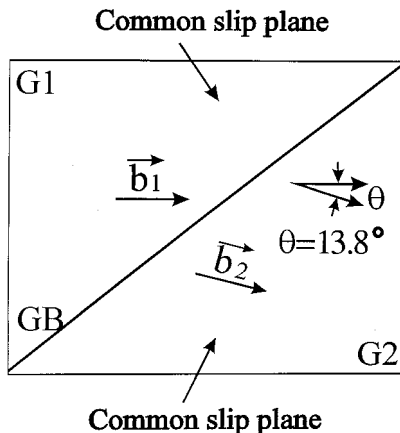


Figure 1. Sketch of slip directions on the common primary slip plane in the copper bicrystal.

Table 1. Parameters of the scanning electron microscope working conditions.

Acceleration voltage (kV)	Working distance (mm)	Filament current (A)	Probe current (A)	Brightness (%)	Contrast (%)	Scanning rate
20	15–20	2–3	2–5	60–75	30–33	TV/2K

embedded within matrix veins throughout the whole specimen, they should alternately appear after repeatedly polishing away the common primary slip plane. The interactions of the GB with the PSB and matrix lamellae can thereby be observed. The ECC technique was carried out in a Cambridge S360 scanning electron microscope. Similar to the image system reported by Schwab *et al.* (1996), an inverted imaging mode was adopted in the present investigation. Thus, the bright areas in the ECC micrograph represent dislocation-poor regions, whereas the dark areas represent dislocation-dense regions, which is in accord with the transmission electron micrograph under bright imaging conditions. The parameters of the scanning electron microscope working conditions are listed in table 1.

### § 3. RESULTS AND DISCUSSION

After cyclic deformation of the bicrystals, the two-phase structure of PSBs and loop patches on the specimen surface is observed in both grains G1 [I34] and G2 [18 2 7], as reported previously (Zhang *et al.* 1999). If the observations are focused on the common primary slip plane in the bicrystal, two kinds of dislocation pattern are found. Figure 2(a) shows the typical dislocation vein structure with some parallel and dislocation-free channels. This observation is in good agreement with that observed on the (111) plane in fatigued copper single crystals (Winter 1978, Laird *et al.* 1986). In particular, those veins appear over the whole observation surface; no dislocation walls can be seen. It is indicated that the observed surface should correspond to the matrix lamellae rather than to PSB lamellae. When the specimen was polished repeatedly to observe the common primary slip plane, another typical dislocation pattern, that is PSB walls embedded within the matrix veins, can be clearly observed, as shown in figure 2(b). The interesting finding is that PSB walls are surrounded by the channels (or veins) and both of those appeared alternately over the whole surface. However, PSB walls extending through the whole surface were not observed. This can be attributed to two main reasons. The first is that the observation plane might not completely correspond to the (111) plane owing to a deviation caused by cutting and polishing procedure. The second might be that there still exists localization of plastic strain even within a single PSB, and PSB walls cannot extend through the whole primary slip plane during cyclic deformation. Similar observations on the (111) plane have been reported previously in copper single crystals (Winter 1978; Laird *et al.* 1986, Basinski and Basinski 1992).

After the specimen was polished further, an interesting finding on the common primary slip plane is that there exists a grain-boundary-affected zone (GBAZ) of dislocation patterns. Such a GBAZ appears in both the G1 [I34] and the G2 [18 2 7] grains. The width of the GBAZ of dislocation patterns within the two grains far from the specimen centre is nearly the same (5–10  $\mu\text{m}$ ), as reported previously (Zhang *et al.* 1999). In appearance, the GBAZ is somewhat similar to the dislocation-free zone (DFZ) in a fatigued [I35]–[I35] copper bicrystal (Hu *et al.* 1998) and in a polycrystal

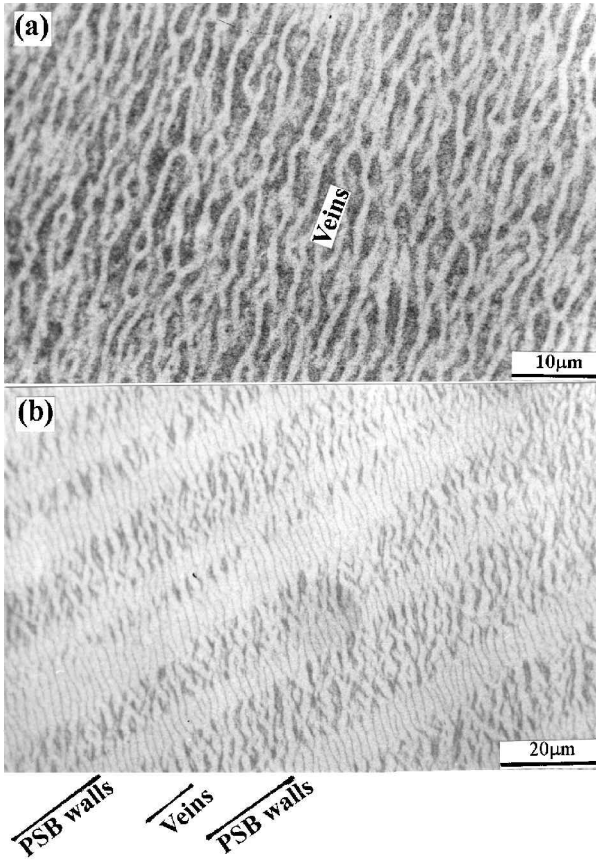


Figure 2. Dislocation patterns in the interior of the grains on the primary slip plane: (a) typical dislocation veins; (b) PSB walls embedded within the matrix veins.

(Louh and Chang 1996). However, close to the specimen centre, the GBAZ gradually became unclear or disappeared, as shown in figure 3 (a). In combination with the previous observations (Zhang *et al.* 1999), a diagrammatic sketch of the GBAZ distribution on the matrix lamellae can be illustrated as in figure 4 (a). However, the formation mechanism of the GBAZ is still not clear and needs to be further clarified.

The above-mentioned interaction of dislocations with the GB mainly corresponds to the matrix lamellae without any PSB walls. As the PSB walls were exposed on the common primary slip plane, it was found that all the dislocation walls reached or were close to the GB. Figure 3 (b) shows one kind of interaction mode between PSB walls and the GB; clearly, the dislocation wall in a PSB within grain G1 can reach the GB and no GBAZ formed between the dislocation walls and the GB. However, on the other side, there is still a GBAZ with a width of 5–10  $\mu\text{m}$ . Meanwhile, the dislocation pattern is typical veins and not regular walls within the grain G2. Another interesting finding is that the GBAZ can nucleate between the PSB walls and the GB, as shown in figure 3 (c). The width of the GBAZ in this case is also similar to that formed in previous observations (5–10  $\mu\text{m}$ ) between the GB and dislocation veins (Zhang *et al.* 1999). It is suggested that the PSB walls may not affect

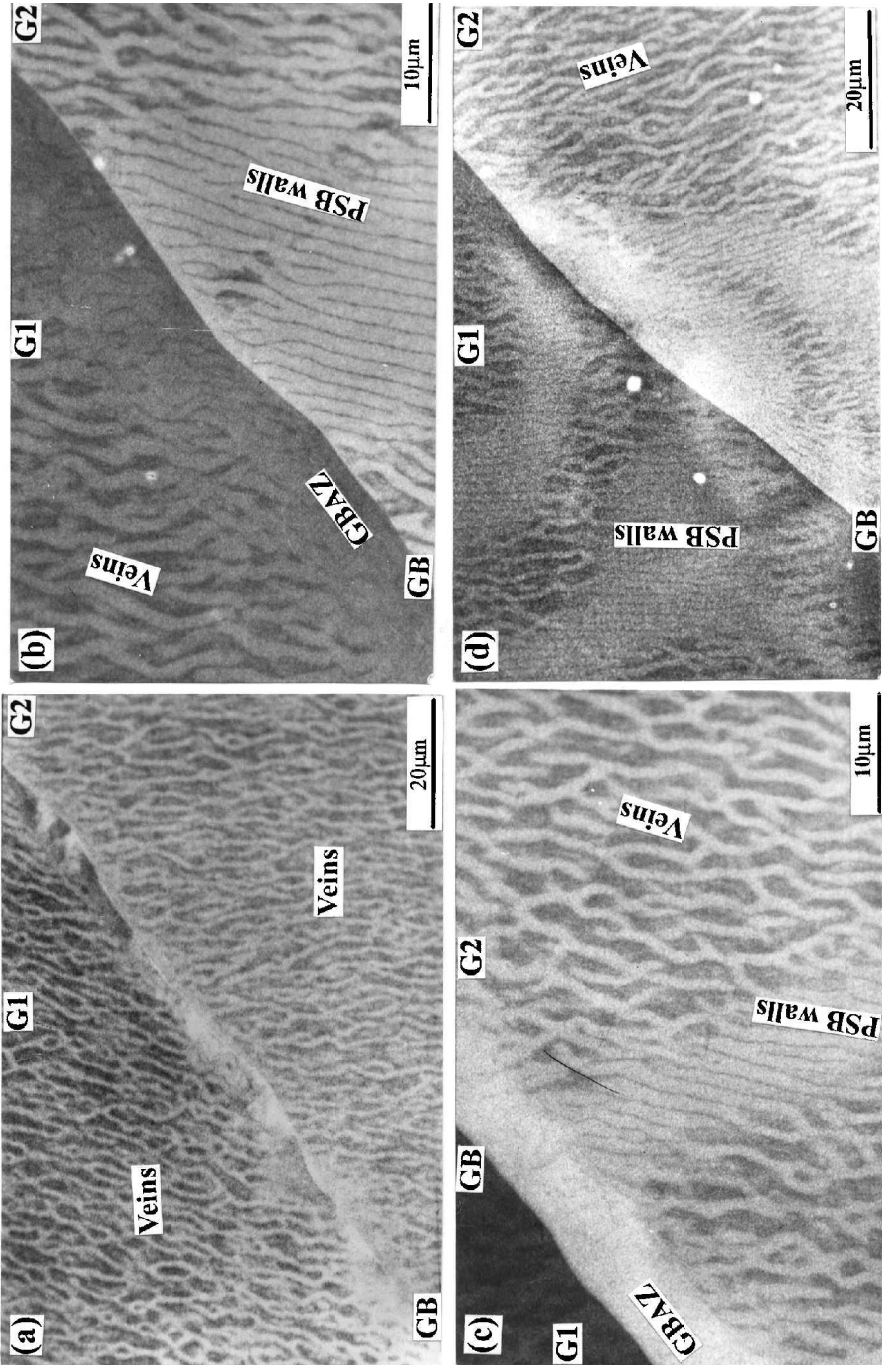


Figure 3. Dislocation patterns near the GB on the primary slip plane; (a) disappearance of the GBAZ in the centre of the specimen; (b), (c) interactions of PSB walls with the GB; (d) two PSB walls intersecting on the same site of the GB.

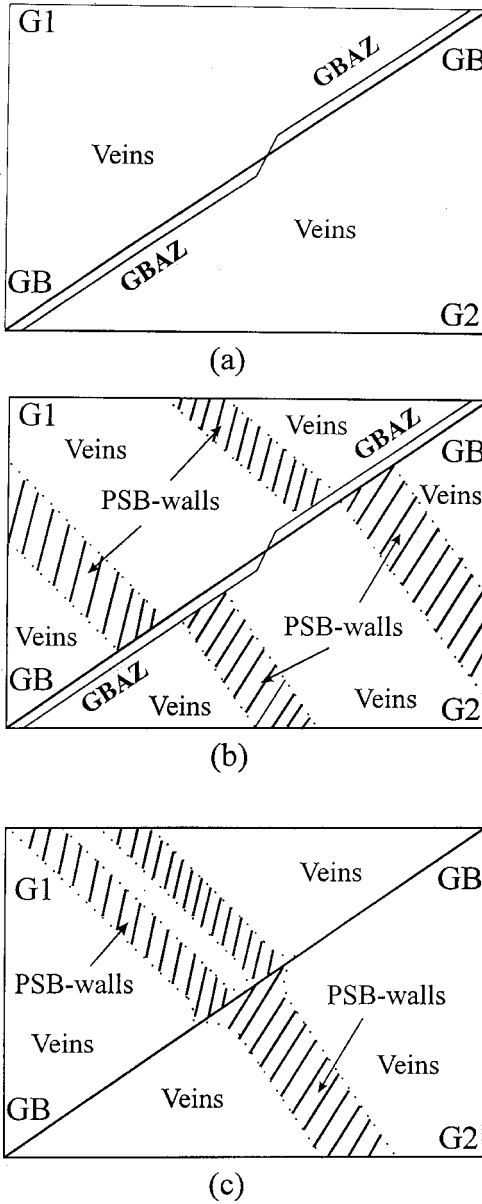


Figure 4. Sketches of three typical interaction modes between the dislocation and the GB.

the formation of the GBAZ during cyclic deformation. From the observations in figures 3 (b) and (c), the typical interaction modes between the GB and PSB walls on the common primary slip plane can be illustrated as in figure 4 (b).

The layer-by-layer observations on the common primary slip plane show that most of the PSBs within the two grains do not have a one-to-one correlation across the GB. Occasionally, the PSBs within the two grains may intersect at the same site of the GB, as shown in figure 3 (d). In this special case, the PSBs are often bent or discontinuous as they are close to the GB. However, the dislocation walls within the

PSBs are still straight and can be clearly distinguished even though they may disappear or become veins in some local regions. The interactions of PSB walls with the GB in this case can be illustrated as in figure 4(c). Note that there seems to exist a stronger interaction of the GB with PSBs than that in figures 3(a)–(c). This can be explained in terms of localization of the plastic strain in the PSB walls during cyclic deformation, especially as the two PSBs within the grains G1 and G2 intersect on the same side of the GB. This may be the reason why the PSBs become bent or discontinuous when they reach the GB.

From the observations above, it is suggested that the PSBs cannot pass through the GB continuously during cyclic deformation even though the two grains have a common primary slip plane. The reason is that their primary slip directions are not the same but have an interaction angle of  $13.8^\circ$ , as shown in figure 1. In particular, there may still exist localization of plastic strain within a single PSB, as shown in figure 2(b), which may strongly interfere with the continuity of the PSB across the GB.

#### § 4. CONCLUSIONS

From the observations above, it can be concluded that the SEM–ECC technique can be successfully applied to investigate the dislocation patterns and the interactions of PSBs with a GB after cyclic deformation. By observing the dislocation patterns on the common primary slip plane in a fatigued  $[\bar{1}34-18\bar{2}7]$  bicrystal layer by layer, the localization of plastic strain may exist even within a single PSB and the PSB walls cannot extend through the whole primary slip plane during cyclic deformation. Near the GB, three kinds of interaction mode of the dislocations with the GB have been identified. All those observations indicate that the PSBs cannot transfer through the GB continuously even though the two grains have a common primary slip plane. The reason is that their primary slip directions are not the same but have an interaction angle of  $13.8^\circ$ . Those observations may provide evidence for a better understanding the intergranular fatigue cracking mechanism.

#### ACKNOWLEDGEMENTS

This work was financially supported by the National Natural Science Foundation of China under grants 59701006 and 19392300-4. The authors are grateful for the support. The authors would like to express their appreciation to Associate Professor H. H. Su for his assistance with the dislocation observations by the SEM–ECC technique.

#### REFERENCES

- AHMED, J., WILKINSON, A. J., and ROBERTS, S. G., 1997, *Phil. Mag. Lett.*, **76**, 237.  
BASINSKI, Z. B., and BASINSKI, S. J., 1992, *Prog. Mater. Sci.*, **36**, 89.  
BRETSCHNEIDER, J., HOLSTE, C., and TIPPELT, B., 1997, *Acta mater.*, **45**, 3755.  
DUDAREV, S. L., AHMED, J., HIRSCH, P. B., and WILKINSON, A. J., 1999, *Acta crystallogr. A*, **55**, 234.  
FINNEY, J. M., and LAIRD, C., 1975, *Phil. Mag. A*, **31**, 339.  
GONG, B., WANG, Z. R., CHEN, D. L., and WANG, Z. G., 1997, *Scripta mater.*, **37**, 1605.  
HU, Y. M., CHEN, D. L., SU, H. H., and WANG, Z. G., 1998, *J. Mater. Sci. Lett.*, **17**, 865.  
LAIRD, C., CHARSLEY, P., and MUGHRABI, H., 1986, *Mater. Sci. Engng*, **81**, 433.  
LI, X. W., HU, Y. M., and WANG, Z. G., 1998, *Mater. Sci. Engng*, **A248**, 299.  
LOUH, T., and CHANG, C. P., 1996, *Acta mater.*, **44**, 2683.  
MELISOVA, D., WEISS, B., and STICKLER, R., 1997, *Scripta mater.*, **36**, 1061.

- MITCHELL, D. R. G., and DAY, R. A., 1998, *Scripta mater.*, **39**, 923.
- SCHWAB, A., BRETSCHNEIDER, J., BUQUE, C., BLOCHWITZ, C., and HOLSTE, C., 1996, *Phil. Mag. Lett.*, **74**, 449.
- SCHWAB, A., MEIßNER, O., and HOLSTE, C., 1998, *Phil. Mag. Lett.*, **77**, 23.
- WILKINSON, A. J., HENDERSON, M. B., and MARTIN, J. W., 1997, *Phil. Mag. Lett.*, **74**, 145.
- WILKINSON, A. J., and HIRSCH, P. B., 1995, *Phil. Mag. A*, **74**, 81; 1997, *Micron*, **28**, 27.
- WINTER, A. T., 1974, *Phil. Mag. A*, **30**, 719; 1978, *ibid.*, **37**, 457.
- ZAUTER, R., PETRY, F., BAYERLEIN, M., SOMMER, C., CHRIST, H.-J., and MUGHRABI, H., 1992, *Phil. Mag.*, A, **66**, 425.
- ZHANG, Z. F., and WANG, Z. G., 1998, *Phil. Mag. Lett.*, **78**, 105.
- ZHANG, Z. F., WANG, Z. G., and SU, H. H., 1999, *Phil. Mag. Lett.*, **79**, 233.